ISSN : 2455-9679
SJIF Impact Factor : 6.190

IJRTSM
INTERNATIONAL JOURNAL OF RECENT TECHNOLOGY SCIENCE & MANAGEMENT

"TRACEABLE TRANSIENT FINITE ELEMENT ASSESSMENT OF AN OFFSHORE CCU LIFTING FRAME UNDER CORNER-FIRST INCLINED DROP IMPACT"

Rohit Shakya [1], Dr. Nitin Tenguria [2], Dr. Syed Faisal Ahmad [3]
[1,2,3] Department of Mechanical Engineering, Sagar Institute of Research & Technology Excellence, Bhopal, Madhya Pradesh, India

ABSTRACT

Offshore cargo-carrying units (CCUs) require lifting frames that can withstand routine handling and short-duration accidental impact. This paper re-examines a supplied finite element study of a welded offshore CCU frame under a corner-first inclined drop condition. Rather than presenting an unverified optimized design, the revised work emphasizes traceability, independent arithmetic checks, response utilization, and a staged verification framework. Source-reported geometry is approximately 155.40 × 95.20 × 107.00 in; the model uses ASTM A500 Grade B tubing, a 26,000 lb payload, a 5,300 lb tare mass, and a reported baseline mesh of 123,667 elements and 115,418 nodes. The reported peak von Mises stress is 28,108 psi, maximum displacement is 0.138 in, and maximum plastic strain is 2.8%. Recalculation gives a stress ratio of 0.611 to the stated 46,000 psi reference and a factor of safety of 1.637. Displacement utilization is 24.0%, 41.4%, and 32.2% of the long-, short-, and corner-member limits. A mass-accounting discrepancy is identified: the stated payload and tare sum to 31,300 lb, not the reported 31,330 lb. The analysis supports a qualified baseline screening conclusion while highlighting that mesh convergence, energy balance, time-step sensitivity, constitutive calibration, and physical validation remain necessary before certification or optimization claims.

Key Words:. *Offshore CCU; lifting frame; corner-first drop; explicit dynamics; finite element analysis; stress utilization; displacement limit; model traceability; validation.*

I. INTRODUCTION

Offshore cargo-carrying units are lifted, transported, positioned, and landed under operational conditions that can include impact, vibration, and non-uniform support. A lifting frame must transfer payload inertia through welded tubular members to the lifting and contact regions. During an inclined drop, the lowest corner contacts the rigid surface first, producing a localized load path before the rest of the structure responds.

The source paper models a CCU lifting frame using ASTM A500 Grade B tubing and evaluates an inclined drop-impact condition using transient finite element analysis. Its reported results indicate that the lower first-contact corner governs peak stress, while the longer base member governs maximum global displacement. These distinct locations demonstrate why a single contour plot or a single scalar metric is not sufficient for structural interpretation.

The purpose of this revision is to create a more traceable assessment of the existing numerical evidence. It does not claim to rerun the original solver, independently verify every material input, or establish certification compliance.

ISSN : 2455-9679
SJIF Impact Factor : 6.190

Instead, it recalculates ratios, checks internal consistency, and identifies the numerical and experimental evidence needed for a stronger publication-grade assessment.

1.1 Research questions

How do the reported stress and displacement compare with the limits used in the source paper?

Are the payload, tare mass, and gross-mass values arithmetically consistent?

What numerical verification and experimental validation are needed before optimization can be claimed?

How can baseline results be communicated without presenting proposed future work as completed results?

1.2 Scope and boundaries

The scope is limited to the reported corner-first inclined impact case. Static lifting certification, fatigue life, corrosion allowance, weld fracture, lifting-set design, and other regulatory checks are not established by the available transient results.

II. Literature Review and Research Gap

The supplied manuscript's literature review covers explicit drop simulation of steel containers, nonlinear impact of deck structures, dropped-object assessment for offshore and subsea systems, impact on pipelines, and structural topology optimization. It also identifies physical drop testing and Digital Image Correlation (DIC) as useful validation approaches. These themes are retained here as the source-derived research context; bibliographic metadata should be checked against publisher records before journal submission.

2.1 Research gap

The principal gap is not the absence of a baseline FE model. It is the lack of a complete, numerically documented chain from input traceability through mesh/time-step convergence, contact and energy checks, experimental correlation, and then quantitative design optimization. The source paper reports mesh quality indicators, but element quality alone does not establish mesh independence. It also recommends time-step sensitivity and validation, while corresponding numerical sensitivity tables and physical measurements are not available in the supplied results.

2.2 Objectives

Reconstruct a traceable summary of the baseline geometry, material, payload, impact setup, and mesh.
Recalculate stress and displacement utilization from source-reported values.
Audit the reported mass figures and identify discrepancies without silently correcting source data.
Propose a verification and validation workflow that must precede optimization claims.

III. Source Data and Modelling Assumptions

3.1 Geometry and member sections

The supplied paper reports overall dimensions of approximately 155.40 in length, 95.20 in width, and 107.00 in height. The displacement assessment uses a 143.40 in long beam, an 83.20 in short beam, and a 107.00 in corner member. The listed sections include 10 × 6 × 0.375 in rectangular tubes for primary frame members, 6 × 6 × 0.375 in square tubes for corner members, 14 × 6 × 0.25 in rectangular tubes for forklift-pocket/handling members, and 4 × 4 × 0.25 in square tubes for top supports.

Model item	Source-reported specification	Role / note
Overall frame	155.40 × 95.20 × 107.00 in	Overall envelope
Primary rectangular tube	10 × 6 × 0.375 in	Base/top frame
Corner square tube	6 × 6 × 0.375 in	Corner members
Handling tube	14 × 6 × 0.25 in	Forklift-pocket members

ISSN : 2455-9679
SJIF Impact Factor : 6.190

Top support tube	4 × 4 × 0.25 in	Top support members
Payload plate	133.40 × 77.20 × 9 in	Inertial representation of carried payload

3.2 Material and mass representation

ASTM A500 Grade B structural tubing is the material reported in the source paper. The model represents a 26,000 lb payload and a frame tare mass of 5,300 lb. The source also reports a gross mass of approximately 31,330 lb (14,211 kg). These values are preserved as reported, while their arithmetic is audited in Section 5.

3.3 Impact setup

The source defines a corner-first inclined drop with a minimum 5° angle, a free-drop height of approximately 2 in (0.0508 m), gravity of 386.22 in/s², and a rigid impact surface. The reported vertical difference between upper and lower corners is approximately 293 mm; combined with the 50 mm drop height, the source reports 343 mm, below its stated 400 mm limit.

3.4 Mesh and numerical controls

The baseline mesh is reported as approximately 123,667 parabolic tetrahedral elements and 115,418 nodes. The source describes element-quality checks, including a localized maximum aspect ratio of 143. Those metrics do not replace mesh convergence. Contact, time-step control, solver duration, material plasticity, and energy histories must be recorded for reproducibility.

IV. RECALCULATION METHOD

This revision uses only reported baseline values and transparent arithmetic. The calculations below are not a substitute for rerunning the finite element model. They are consistency and utilization checks that can be independently reproduced.

4.1 Stress ratio and factor of safety

Using the reported peak von Mises stress σ_{max} = 28,108 psi and the source's reference strength σ_{ref} = 46,000 psi:

Stress utilization = $\sigma_{max} / \sigma_{ref}$ = 28,108 / 46,000 = 0.6110, or 61.1%.

Arithmetic factor of safety = $\sigma_{ref} / \sigma_{max}$ = 46,000 / 28,108 = 1.637. This agrees with the source's reported value of approximately 1.63.

4.2 Displacement utilization

The source reports a maximum displacement of 0.138 in and member-specific allowable displacements of 0.574 in, 0.333 in, and 0.428 in. Utilization is calculated as computed displacement divided by the corresponding allowable value.

Member	Reported displacement (in)	Allowable (in)	Recalculated utilization	Remaining margin (in)
Long beam	0.138	0.574	24.0%	0.436
Short beam	0.138	0.333	41.4%	0.195
Corner beam	0.138	0.428	32.2%	0.290

4.3 Ideal free-fall velocity check

For a drop height h = 0.0508 m, the ideal velocity immediately before contact is $v = \sqrt{(2gh)} = \sqrt{(2 \times 9.81 \times 0.0508)}$ = 0.998 m/s. This is a kinematic estimate, not a solver-extracted contact velocity; it neglects any setup-specific constraints or numerical effects.

ISSN : 2455-9679
SJIF Impact Factor : 6.190

4.4 Derived metric limitations

Derived ratios inherit the assumptions and definitions of the source values. In particular, the 46,000 psi reference is treated as the criterion used by the supplied paper, not independently certified as the correct material-specific design allowable for every section and loading condition.

V. RESULTS

5.1 Stress-reference comparison

The source reports a maximum von Mises stress of 28,108 psi at the lowest corner contacting the rigid surface first. Against the source's 46,000 psi reference, the recalculated utilization is 61.1% and the arithmetic factor of safety is 1.637. This supports the source's stated baseline stress-screening result, subject to the limitations of the FE model and reference criterion.

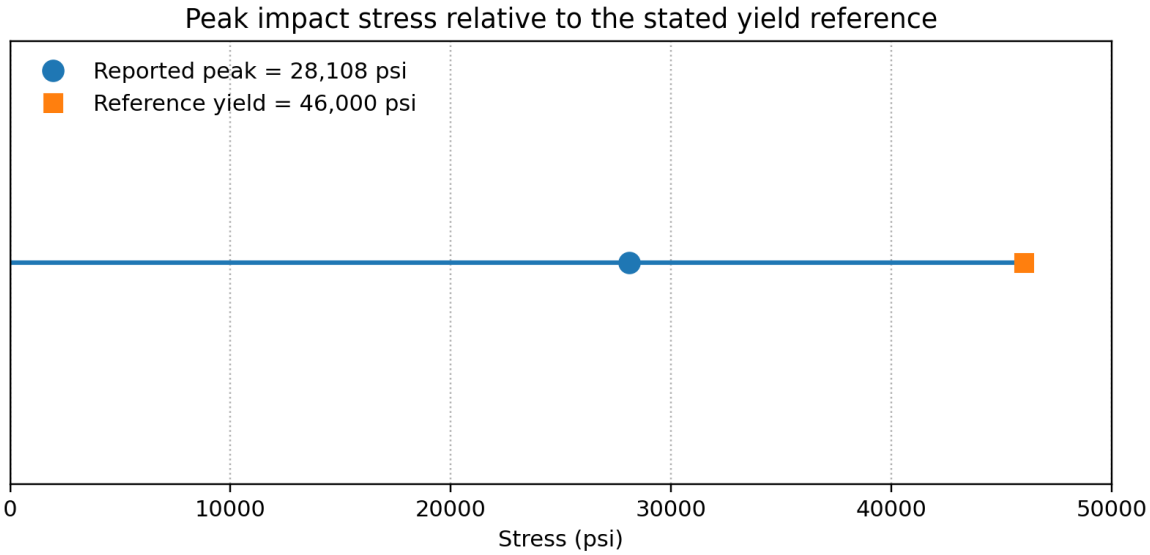


Figure 2. Stress-reference dot plot; both values are source-derived, while the ratio is recalculated.

5.2 Displacement utilization

The reported displacement is 0.138 in for each of the three member checks. The highest utilization is for the short beam at 41.4% of its listed allowable displacement; the long beam has the lowest utilization at 24.0%. These values are recalculated from the source table and should not be confused with new simulation outputs.

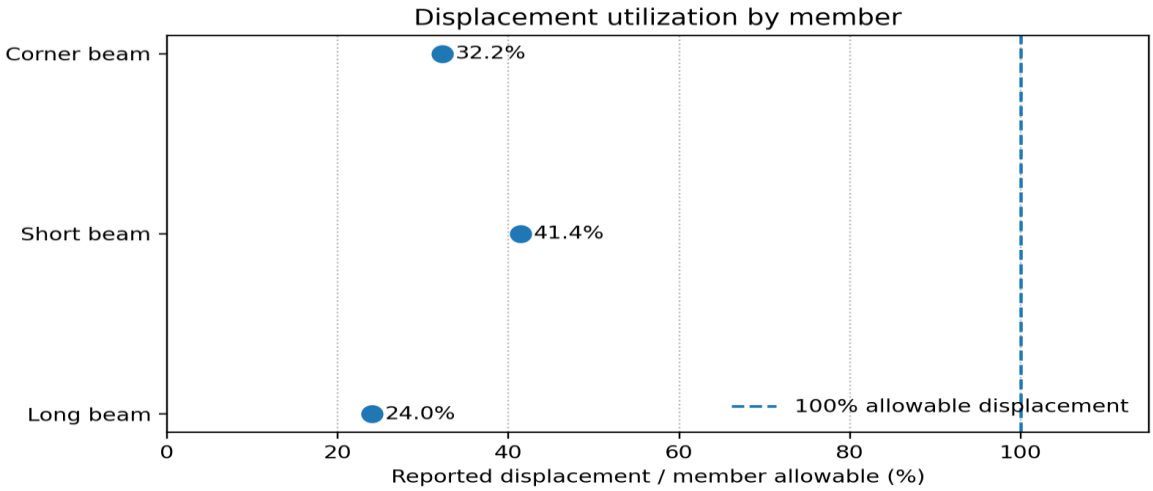


Figure 3. Displacement utilization by member, calculated from reported displacement and allowable values.

ISSN : 2455-9679
SJIF Impact Factor : 6.190

5.3 Mass-accounting audit

The source lists a payload of 26,000 lb and a frame tare mass of 5,300 lb. Their sum is 31,300 lb. The paper separately reports gross mass as 31,330 lb, a difference of 30 lb. Using 1 lb = 0.45359237 kg, the sum converts to 14,197.4 kg, whereas the source reports 14,211 kg. The source values should be checked against the model's mass properties before the paper is finalized.

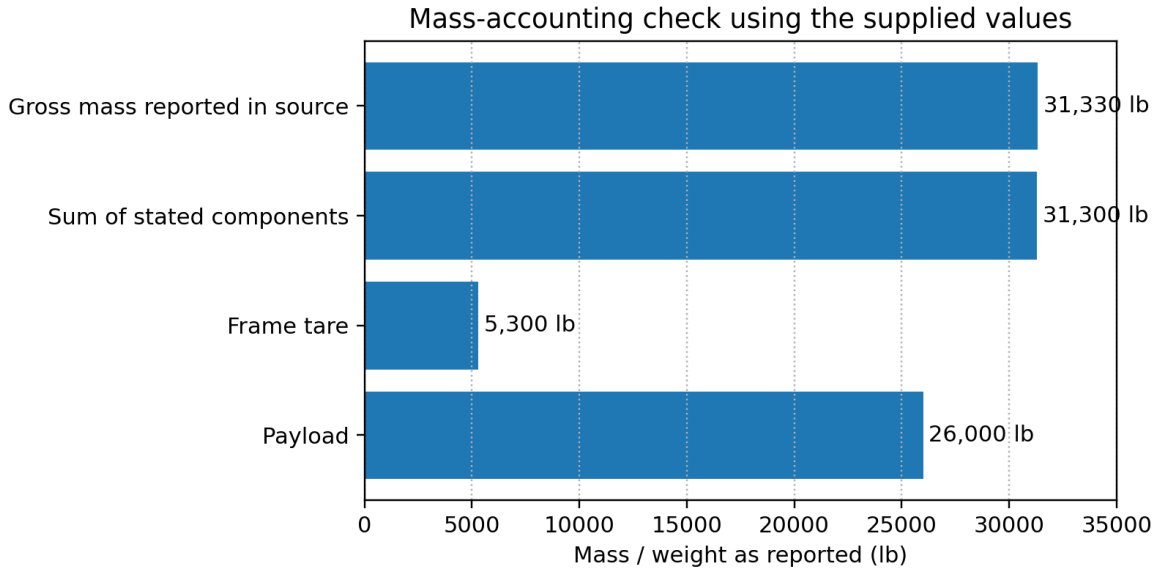


Figure 4. Mass-accounting check; bars reproduce source values and the arithmetic sum.

VI. Discussion

6.1 Local stress versus global displacement

The first-contact lower corner is the reported peak-stress location, which is consistent with sequential contact in an inclined drop. The maximum displacement is reported on the inside of the longer base beam. This difference is mechanically plausible: the impact corner concentrates the initial contact load, while the frame's longer members participate in global bending and load redistribution. The assessment therefore needs local stress/strain and global displacement measures.

6.2 What the baseline results establish

The reported stress and displacement values pass the screening comparisons defined in the source paper. The reported maximum plastic strain is 2.8%, below the paper's study-specific 5% interpretive threshold. That 5% threshold is not presented here as a universal DNV limit; it is retained only as a source-defined screening value. No claim of complete regulatory certification follows from these checks alone.

6.3 What the baseline results do not establish

Mesh independence: element count and quality checks do not show how peak response changes with refinement.
Time-step independence: no numerical time-step sensitivity table is supplied.
Energy balance: kinetic, internal, contact, and hourglass/artificial energy histories are not included in the source values summarized here.
Constitutive validity: strain-rate effects and plasticity calibration are not independently verified.
Physical validation: no strain-gauge or DIC measurements for this exact frame are provided.
Optimized performance: the supplied paper does not provide a quantified post-optimization model.

6.4 Mass discrepancy and reporting discipline

The 30 lb discrepancy between the component sum and reported gross mass is small relative to the total, but it matters for traceability in a research paper. It should be resolved by checking whether the tare mass, payload mass, or gross-

ISSN : 2455-9679
SJIF Impact Factor : 6.190

mass conversion was rounded or transcribed differently. This revision intentionally reports the discrepancy rather than silently replacing the source value.

VII. CONCLUSION

The supplied baseline study reports a corner-first inclined drop-impact analysis of an offshore CCU lifting frame made from ASTM A500 Grade B structural tubing.

The reported peak von Mises stress is 28,108 psi. Against the source's 46,000 psi reference, recalculated utilization is 61.1% and arithmetic factor of safety is 1.637.

The reported maximum displacement of 0.138 in corresponds to 24.0%, 41.4%, and 32.2% of the long-, short-, and corner-member allowable values, respectively.

The reported maximum plastic strain is 2.8%, below the source's study-specific 5% screening threshold; this is not interpreted as a universal standard limit.

The stated payload and tare mass sum to 31,300 lb, which differs from the source-reported gross mass of 31,330 lb. This discrepancy and its kilogram equivalent require confirmation from the model data.

Mesh convergence, time-step sensitivity, energy balance, constitutive calibration, and physical correlation remain unreported or incomplete in the supplied evidence.

No quantitative optimization result is claimed. Optimization should follow verification and validation and should be reported with baseline-to-candidate comparisons.

REFERENCES

[1] Protz, C., Zencker, U., & Liebich, R. (2015). Explicit finite element analyses of drop tests with thin-walled steel sheet containers for the Konrad repository.

[2] Jung, B.-G., Jo, S.-W., Noh, S.-H., Paik, J. K., Seo, J., & Kim, Y. (2016). Experimental and numerical studies on nonlinear impact response of deck structures subjected to dropped objects.

[3] Kwon, Y.-J. (2017). Comparative study of finite element analysis for stresses occurring in various models of the spent nuclear fuel disposal canister due to accidental drop and impact onto the ground.

[4] Woo, S.-H., Lee, K.-S., & Jeong, J.-M. (2017). Design of deep-sea manifold protective structure considering dropped-object impact.

[5] Othman, H., Sabrah, T., & Marzouk, H. (2017). Feasibility of using ultra-high performance fiber reinforced concrete for radioactive waste containers: Drop test simulation.

[6] Lu, Y., Sun, L., Zhang, X., Kang, J., Zhang, Q., & Yu, B. (2018). Analysis of FPSO dropped objects combining Monte Carlo simulation and neural network-genetic approach.

[7] Ozguc, O. (2019). Structural assessment of the hull response of an FPSO unit to dropped objects: A case study.

[8] Jiang, F., Dong, S., Zhao, Y., Xie, Z., & Guedes Soares, C. (2019). Investigation on the deformation response of submarine pipelines subjected to impact loads by dropped objects.

[9] Lin, M., & Li, Y. (2020). Analysis of the interactions between spent fuel pebble bed and storage canister under impact loading.

[10] Deng, W., Tian, X., Han, X., Liu, G., Xie, Y., & Li, Z. (2021). Topology optimization of jack-up offshore platform leg structure.

[11] Ozguc, O. (2021). The assessment of impact damage caused by dropped objects on floating offshore structures.

[12] Lee, K., & Ryu, H. (2021). Dropped object impact analysis considering frequency and consequence for LNG-FPSO topside module.

[13] Tian, X., Sun, X., Liu, G., Deng, W., Wang, H., Li, Z., & Li, D. (2022). Optimization design of the jacket support structure for offshore wind turbine using topology optimization method.

[14] Tian, X., Wang, Z., Liu, D., Liu, G., Deng, W., Xie, Y., & Wang, H. (2022). Jack-up platform leg optimization by topology optimization algorithm-BESO.

ISSN : 2455-9679
SJIF Impact Factor : 6.190

[15] Zhang, C., Long, K., Zhang, J., Lu, F., Bai, X., & Jia, J. (2022). A topology optimization methodology for the offshore wind turbine jacket structure in the concept phase.
[16] Shrivastava, A. K., Sinha, A. K., Choubey, A., Choubey, N., Billore, M., & Qureshi, J. H. (2023). Drop test finite element analysis of different grades of ASTM A500 for structural lifting frame.
[17] Oka, J. M., Vaidya, R. U., Davis, J. T., Webber, K. W., & Walzel, R. K. (2024). Nuclear material container drop testing using finite element analysis with verification using digital image correlation.
[18] Tuswan, T., Andrian, M., Amiruddin, W., Muttaqie, T., Sari, D. P., Bisri, A., Yuniati, Y., Soetarjo, M., Utina, M. R., & Harmadi, R. (2024). Design improvement using topology optimization for the structural frame design of a 40 ft LNG ISO container tank.
[19] Chae et al. (2024). Machine learning-aided damage identification of mock-up spent nuclear fuel assemblies in a sealed dry storage canister.
[20] Lin et al. (2024). Recent numerical/experimental container-impact research relevant to high-strain drop response.
[21] Residual-strength study on container ships subjected to dropped-container impact. (2025). Residual ultimate strength of a container ship under dropped-object impact: Numerical simulations and empirical formulations.
[22] Study on duplex stainless steel in drop scenarios for dry-storage containers. (2025). Dynamic behavior of duplex stainless steel with improved chloride-induced stress corrosion cracking resistance in drop scenarios for dry storage containers.
[23] Roh, H., Ra, C., & Park, N. C. (2026). Finite-element analysis methodology for sequential impact events of dry storage containers.
[24] Drozdowski, J., & Niklas, K. (2026). Structural multi-objective optimization of the offshore jacket structure through rule-based buckling integrated with finite element analysis.